

Comparison of Radiolabeled Nucleoside Probes (FIAU, FHBG, and FHPG) for PET Imaging of HSV1-*tk* Gene Expression

Juri Gelovani Tjuvajev, MD, PhD^{1,2}; Mikhail Doubrovin, MD, PhD¹; Timothy Akhurst, MD^{2,3}; Shangde Cai, PhD⁴; Julius Balatoni, PhD¹; Mian M. Alauddin, PhD⁵; Ronald Finn, PhD^{2,4}; William Bornmann, PhD⁶; Howard Thaler, PhD⁷; Peter S. Conti, MD⁵; and Ronald G. Blasberg, MD^{1,2}

¹Department of Neurology, Memorial Sloan-Kettering Cancer Center, New York, New York; ²Department of Radiology, Memorial Sloan-Kettering Cancer Center, New York, New York; ³Nuclear Medicine Service, Memorial Sloan-Kettering Cancer Center, New York, New York; ⁴Radiochemistry/Cyclotron Core Facility, Memorial Sloan-Kettering Cancer Center, New York, New York; ⁵Department of Radiology, PET Imaging Science Center, University of Southern California, Los Angeles, California; ⁶Preparative Core Resource Facility, Memorial Sloan-Kettering Cancer Center, New York, New York; and ⁷Department of Epidemiology and Biostatistics, Memorial Sloan-Kettering Cancer Center, New York, New York

The efficacy of 3 radiolabeled probes of current interest for imaging herpes simplex virus type 1 thymidine kinase (HSV1-*tk*) expression in vivo with PET, including ¹²⁴I- or ¹³¹I-labeled 2'-fluoro-2'-deoxy-1-β-D-arabinofuranosyl-5-iodouracil (FIAU), ¹⁸F-labeled 9-[4-fluoro-3-(hydroxymethyl)butyl]guanine (FHBG), and ¹⁸F-labeled 9-[3-fluoro-1-hydroxy-2-propoxymethyl]guanine (FHPG), was compared. **Methods:** Two established rat glioma cell lines, stably transduced RG2TK+ and wild-type RG2, were used for paired comparisons of probe accumulation in vitro and for paired comparisons of subcutaneous xenografts produced from these cell lines in athymic *nu/nu* rats. **Results:** The in vitro paired probe uptake (0–3 h) comparisons in RG2TK+ cells showed that FIAU accumulation was 15-fold greater than that of FHBG and 41-fold greater than that of FHPG. The net accumulation rate values (±SD) calculated for RG2TK+ cells were 0.317 ± 0.066, 0.022 ± 0.001, and 0.0077 ± 0.0003 mL/min/g cells for FIAU, FHBG, and FHPG, respectively. These results and similar uptake studies in RG2 wild-type cells suggest a possible cell membrane transport limitation for FHBG and FHPG. The paired 2-h in vivo uptake studies produced similar differences in RG2TK+ xenografts for FIAU and FHBG (1.22 ± 0.21 vs. 0.074 ± 0.49 %dose/g) and for FIAU and FHPG (1.27 ± 0.14 vs. 0.023 ± 0.008 %dose/g). These differences were clearly visible on the images. FIAU accumulation at 24 h was 1.53 ± 0.40 %dose/g. Plasma clearance was FHBG > FHPG >> FIAU. The FIAU images showed significant stomach and some intestinal background radioactivities, whereas hepatobiliary and intestinal background activities were very high for the guanosine analogs (FHBG > FHPG). Dynamic imaging showed early (~10 min) selective localization of FIAU in RG2TK+ xenografts, whereas FHBG and FHPG are being cleared from the HSV1-*tk* transduced and wild-type xenografts over the initial 2-h imaging period. **Conclusion:** The in

vitro and in vivo results (including the PET images) show that FIAU is a substantially more efficient probe than FHBG or FHPG for imaging HSV1-*tk* expression, with greater sensitivity and contrast as well as lower levels of abdominal background radioactivity at 2 and 24 h.

Key Words: HSV1-*tk*; PET; 2'-fluoro-2'-deoxy-1-β-D-arabinofuranosyl-5-iodouracil; 9-[3-fluoro-1-hydroxy-2-propoxymethyl]guanine; 9-[4-fluoro-3-(hydroxymethyl)butyl]guanine; ¹²⁴I; ¹⁸F; reporter gene

J Nucl Med 2002; 43:1072–1083

In the initial series of articles by Tjuvajev et al. (1–3), a paradigm for noninvasive imaging of transgene expression was described that requires the appropriate combination of a reporter gene and a reporter substrate or probe. This imaging paradigm is essentially an in vivo radiotracer enzyme assay, where the reporter gene product (an enzyme) selectively converts a reporter probe to a metabolite that is trapped within the transduced cell. Model systems have been established and validated in tissue culture and in experimental animals using the herpes simplex virus type 1 thymidine kinase (HSV1-*tk*) gene as a reporter gene and radiolabeled 2'-fluoro-2'-deoxy-1-β-D-arabinofuranosyl-5-iodouracil (FIAU) as a reporter probe (1). Highly specific images of HSV1-*tk* expression in experimental animal tumors were obtained noninvasively using radioiodinated ¹³¹I-FIAU and a clinical gamma-camera system (2,4,5) or ¹²⁴I-FIAU and PET (3,6,7).

This paradigm and the use of reporter gene technology had been extended into several different realms. Reporter genes can be used to image vector targeting and the level of suicide gene (HSV1-*tk*) expression (5), to image the regulation of endogenous genes and signal-transduction pathways (6–8), and to monitor and quantitatively assess the

Received Oct. 25, 2001; revision accepted Mar. 25, 2002.
For correspondence or reprints contact: Ronald G. Blasberg, MD, Department of Neurology, Room K923, Memorial Sloan-Kettering Cancer Center, 1275 York Ave., Box 52, New York, NY 10021.
E-mail: Blasberg@neuro1.mskcc.org

expression of a second transgene that is *cis*-linked to the reporter gene by an internal ribosome entry site sequence (4,9).

Other radiolabeled probes for imaging HSV1-*tk* expression and other reporter genes using radiolabeled probes for non-invasive PET imaging have been developed. For example, 9-[(2-hydroxy-1-(hydroxymethyl)ethoxy)methyl]guanine (GCV) and 9-[4-hydroxy-3-(hydroxymethyl)butyl]guanine (PCV) (10–15) and other ^{18}F -labeled acycloguanosine analogs, such as 8-fluoro-9-[(2-hydroxy-1-(hydroxymethyl)ethoxy)methyl]guanine (FGCV) (12,13), 8-fluoro-9-[4-hydroxy-3-(hydroxymethyl)butyl]guanine (FPCV) (14,15), 9-[3-fluoro-1-hydroxy-2-propoxymethyl]guanine (FHPG) (16,17), and 9-[4-fluoro-3-(hydroxymethyl)butyl]guanine (FHBG) (18) have been developed as reporter substrates for imaging wild-type and mutant (14) HSV1-*tk* expression. Recently, imaging, pharmacokinetics, and dosimetry of ^{18}F -FHBG were reported in healthy volunteers as a preface to imaging HSV1-*tk* reporter expression in clinical gene therapy trials (19).

The objective of this study was to compare the efficacy of 3 radiolabeled probes (FIAU, FHBG, and FHPG) for in vivo imaging of HSV1-*tk* expression with PET. The experimental design of the in vitro and in vivo studies provides for paired comparisons between FIAU and FHBG and between FIAU and FHPG. The PET studies and comparisons were also performed on the same animals. Our results show that FIAU is a substantially better probe than either FHBG or FHPG for imaging HSV1-*tk* expression, with greater sensitivity and lower abdominal background radioactivity at 2 and 24 h.

MATERIALS AND METHODS

Cell Lines

RG2 rat glioma cell line was kindly provided by Dr. Darell Bigner (Duke University Medical Center, Durham, NC). RG2 cells were transduced with the recombinant replication-deficient STK retrovirus containing the *NeoR* gene and HSV1-*tk* gene as described (1). The transduced cell line, RG2TK+, has remained stable and has expressed constant levels of HSV1TK+ since 1994; this cell line has been characterized previously (1,2).

^{18}F -FHBG and ^{18}F -FHPG Syntheses

The syntheses of ^{18}F -FHBG and ^{18}F -FHPG were performed with minor modifications according to procedures reported in the literature (16–18). Briefly, 3.7 GBq (100 mCi) of no-carrier-added aqueous H^{18}F from the cyclotron target was added to a solution of potassium carbonate (2–3 mg) and Kryptofix 2.2.2. (12–15 mg; Aldrich Chemical Co., Milwaukee, WI) in CH_3CN and H_2O (88:12). Azeotropic distillation at 115°C with freshly distilled acetonitrile (3×1 mL) under a nitrogen stream efficiently removed the target H_2O . N^2 -(*p*-Anisylidiphenylmethyl)-9-[(4-tosyl)-3-*p*-anisylidiphenylmethoxymethylbutyl]guanine (16–18) (3–4 mg dissolved in 0.5 mL of freshly distilled acetonitrile) was introduced to the anhydrous potassium fluoride-Kryptofix 2.2.2. complex. The reaction mixture was heated at 120°C for 20 min and was subsequently allowed to cool, at which time the crude product was

passed through a silica Sep-Pak cartridge to remove Kryptofix 2.2.2. and nonreacted fluoride. The Sep-Pak was eluted with 15% methanol/dichloromethane (3.5 mL) and evaporated in vacuo. The residue was acidified with 1N HCl (0.6 mL) and heated for 10 min at 120°C . Upon cooling, the contents were neutralized with 6N NaOH (0.1 mL). The crude product was purified by high-performance liquid chromatography (HPLC) on a semipreparative column (Luna C-18, 10×250 mm; Alltech Associates, Inc., Deerfield, IL). The mobile phase consisted of 5% EtOH/ H_2O and the flow rate was set at 5 mL/min. ^{18}F -FHBG eluted at 12 min under these conditions. ^{18}F -FHPG was prepared similarly from N^2 -(*p*-anisylidiphenylmethyl)-9-[(1-anisylidiphenyl)-3-tosyl-2-propoxymethyl]guanine (16–18) and was purified under the same conditions as described above; ^{18}F -FHPG eluted at 7 min.

The radiochemical purities of ^{18}F -FHBG and ^{18}F -FHPG were $>97\%$ as measured by radio-HPLC using an analytic Luna C-18 column (4.5×250 mm) and 6% acetonitrile/ H_2O as the mobile phase. For specific activity calculations, standard solutions of each compound were injected to the HPLC column, and the area under ultraviolet (UV) was measured. The radioactive product with known activity was injected to the HPLC column under the same condition, and the area under UV was measured. This area under the UV peak was converted to mass, and activity was divided by the mass to yield specific activity for that preparation (16). In our previous studies we reported the estimated lower limits of specific activities of ^{18}F -FHBG and ^{18}F -FHPG to be 11.8 GBq/ μmol (320 Ci/mmol) (18) and 19.5 GBq/ μmol (526 Ci/mmol) (16), respectively. In more recent experiments, we found that a small amount of UV active impurity elutes close to the product. We initially thought this peak represented unlabeled product; however, this was subsequently determined to be incorrect. Therefore, a more likely estimate of the specific activity for ^{18}F -FHBG and ^{18}F -FHPG used in these experiments is in the range of 44.4–74.0 GBq/ μmol (1,200–2,000 Ci/mmol) (although this was not determined at the time the syntheses were performed for the studies reported in this article). The final product was tested for sterility and pyrogenicity by standard techniques and found to be sterile and free from pyrogens.

In Vitro Assays

RG2TK+ and RG2 cells in culture were used to compare the accumulation of ^{14}C -FIAU (2.07 GBq/mmol [56 mCi/mmol], $>99.7\%$ radiochemical purity; Moravak Biochemicals, Brea, CA) and each of the guanosine analogs, ^{18}F -FHBG and ^{18}F -FHPG, as described (1). Paired time-course radiotracer accumulation experiments were run over 180 min and the data were normalized to ^3H -thymidine ([TdR] 2,220 GBq/mmol [60 Ci/mmol], $>99.5\%$ radiochemical purity; Moravak Biochemicals) accumulation. The incubation medium contained ^{14}C -FIAU (0.37 kBq/mL [0.01 μCi /mL], 0.18 μmol /L), ^{18}F -FHBG (148 kBq/mL [4 μCi /mL], 7.6 pmol/L), or ^{18}F -FHPG (148 kBq/mL [4 μCi /mL], 12.5 pmol/L) and ^3H -TdR (3.7 kBq/mL [0.1 μCi /mL], 0.16 pmol/L). The radioactivity assay for the in vitro tissue culture studies involved ^{18}F γ -counting (AutoGamma 5550 spectrometer; Packard Instruments, Meriden, CT) immediately after the experiment, followed 24–36 h later by ^3H and ^{14}C β -isotope counting (Tri-Carb Liquid Scintillation Analyzer, model 1600TR; Packard Instruments) using external standard quench correction and standard dual-counting techniques. All data were expressed as disintegrations per minute (dpm)/g cells (or dpm/mL medium). The net accumulation rate (*K*) was calculated from the slope of the probe accumulation versus

time plot (dpm/g cells \div dpm/mL medium vs. time; units = mL medium/g cells/min – a clearance constant).

¹²⁴I-FIAU Synthesis

¹²⁴I-FIAU was synthesized as described (6) with some modifications. Briefly, ¹²⁴I was produced on the Memorial Sloan-Kettering Cancer Center (MSKCC) CS-15 cyclotron using the ¹²⁴Te(p,n)¹²⁴I nuclear reaction on an enriched ¹²⁴TeO₂/Al₂O₃ solid target (20). The 2'-fluoro-2'-deoxy-1-β-D-arabinofuranosyl-5-(tri-*n*-butyltin)-uracil (FTBSnAU) precursor was prepared by an adaptation of a procedure by Vaidyanathan et al. (21) in 69% yield and was identified by ¹H and ¹⁹F nuclear magnetic resonance spectroscopy and mass spectrometry. Na¹²⁴I was added to a solution of FTBSnAU (125 μg) dissolved in 50 μL methanol, followed by the addition of a 20-μL mixture of 30% hydrogen peroxide/acetic acid (1:3, v/v). Aqueous saturated sodium metabisulfate (0.1 mL) was added to quench the reaction; then the reaction mixture was loaded onto a C₁₈ Sep-Pak cartridge system (Waters, Milford, MA). The C₁₈ cartridge system was eluted with water (35 mL), followed by methanol (3–4 mL) to isolate the ¹²⁴I-FIAU. The methanol was evaporated and the ¹²⁴I-FIAU was formulated in physiologic saline (with 5% ethanol added), which was passed through a sterile 0.22-μm Millipore filter (Millipore, Inc., Bedford, MA).

The radiochemical purity was determined by radio-thin-layer chromatography (silica gel plates [Sigma-Aldrich, St. Louis, MO]; eluent, ethyl acetate/acetone/H₂O, 14:8:1). ¹²⁴I-FIAU comigrated with authentic FIAU standard. The radiolabeled product was isolated in 51%–54% radiochemical yield (3 labelings), with radiochemical purities of $\geq 97\%$. The specific activity of the initial Na¹²⁴I was found to be $> 1,110$ GBq/μmol (> 30 Ci/μmol) (20), so that the specific activity of the ¹²⁴I-FIAU was estimated to be similar to this value. The structure of FIAU was confirmed by single-crystal x-ray analysis.

¹³¹I-FIAU Synthesis

No-carrier-added ¹³¹I-FIAU was prepared by the same iodo-desannylation method (21) as was used for ¹²⁴I-FIAU. Commercially produced Na¹³¹I was obtained from New England Nuclear (North Billerica, MA). Radiochemical yields obtained with ¹³¹I averaged 93% (3 labelings), and radiochemical purities were found to be $\geq 99\%$. The specific activities of the ¹³¹I-FIAU produced were estimated to be 48–59 GBq/μmol (1.3–1.6 Ci/μmol) on the basis of the manufacturer's specifications accompanying the Na¹³¹I lots used.

Subcutaneous Xenografts and Animal Studies

The experimental protocol involving animals was approved by the Institutional Animal Care and Use Committee of MSKCC. Subcutaneous xenografts were produced in *rnu/rnu* rats (Frederick Cancer Center, Frederick, MD) weighing 200–250 g by subcutaneous injection of 5×10^6 tumor cells in 200 μL of serum-free cell culture medium under anesthesia (ketamine [87 mg/kg] and xylazine [13 mg/kg], intraperitoneally). Transduced RG2TK+ cells were placed in the left shoulder (test) and wild-type RG2 cells were placed in the right shoulder (negative control). The animals were monitored for tumor growth by daily measurements of the tumor's size and the animal's weight. Animals were studied when the subcutaneous tumor xenografts reached a diameter of ~ 15 mm, 7–14 d after subcutaneous implantation of the RG2 and RG2TK+ cells. The *in vivo* growth rate, macroscopic and micro-

scopic appearances, and the degree of vascularization were similar in the HSV1-*tk* transduced and wild-type subcutaneous xenografts.

Three days before study, all animals received 1.0-mL intravenous injections of a 0.9% NaI solution (30 mg/kg NaI) daily for 3 consecutive days to block thyroid uptake of radioactive iodide. For the paired 2-h FHBG–24-h FIAU imaging studies ($n = 6$), the animals were first injected with ¹⁸F-FHBG (27.8 MBq [0.75 mCi] per animal intravenously), imaged over 2 h, and then injected with ¹²⁴I-FIAU (8.9 MBq [0.24 mCi] per animal intravenously) and reimaged 24 h later. For the paired 2-h FHPG–24-h FIAU imaging studies ($n = 6$), the animals were first injected with ¹⁸F-FHPG (61.1 MBq [1.65 mCi] per animal intravenously), imaged over 2 h, and then injected with ¹²⁴I-FIAU (13.0 MBq [0.35 mCi] per animal intravenously) and reimaged 24 h later. For the paired 2-h FHBG–2-h FIAU imaging studies ($n = 6$), the animals were first injected with ¹⁸F-FHBG (50.0 MBq [1.35 mCi] per animal intravenously) and imaged over 2 h; 24 h later the same animals were injected with ¹²⁴I-FIAU (7.0 MBq [0.19 mCi] per animal intravenously) and reimaged over 2 h. Immediately after the ¹²⁴I-FIAU imaging sessions, animals were euthanized and tissue samples were processed for ¹²⁴I radioactivity using an AutoGamma 5550 spectrometer (Packard Instruments). Radioactivity is expressed as percentage dose/g tissue (%dose/g tissue).

For the paired 2-h ¹³¹I-FIAU–¹⁸F-FHBG and the 2-h ¹³¹I-FIAU–¹⁸F-FHPG tissue sampling studies, 2 groups of animals were studied. Simultaneous intravenous injection of ¹³¹I-FIAU (1.81 MBq [0.049 mCi] per animal) and ¹⁸F-FHPG (14.8–25.9 MBq [0.40–0.70 mCi] per animal) was performed in 1 group ($n = 6$), and injection of ¹³¹I-FIAU (3.18 MBq [0.086 mCi] per animal) and ¹⁸F-FHBG (5.55–13.0 MBq [0.15–0.35 mCi] per animal) was performed in the other group ($n = 6$). All animals were euthanized at 2 h after injection, and the tissue samples were processed for ¹³¹I and ¹⁸F radioactivity assay using an AutoGamma 5550 spectrometer. The upward cross-talk of ¹³¹I into the ¹⁸F channel was 2.7% of the counts in the ¹³¹I channel. Corrections for ¹⁸F and ¹³¹I decay and ¹³¹I upward cross-talk were applied to all samples. Radioactivity in the animal studies is expressed as %dose/g tissue.

PET

PET imaging was performed using the Advance Tomograph (General Electric Medical Systems, Milwaukee, WI), with a spatial resolution of 5-mm full width at half maximum (FWHM) at the center of the field of view. This camera was cross-calibrated previously with the AutoGamma 5550 spectrometer. All animals were anesthetized with ketamine (87 mg/kg) and xylazine (13 mg/kg) administered intraperitoneally. Measured attenuation correction was performed using a 7-min-duration transmission scan with two 107.3-MBq (9 mCi) germanium transmission sources. Two-dimensional emission scans were obtained for all studies.

Four studies ($n = 6$ animals per study) acquired dynamic image data from 10 or 20 min to 130 min after injection; acquisition frames were either 10 or 20 min in duration, depending on the dose of radiopharmaceutical administered. Two studies ($n = 6$ animals per study) involved imaging at 24 h after injection of ¹²⁴I-FIAU (20-min acquisition).

Emission counts were corrected for random coincidences, dead time, and scatter. Emission scans were reconstructed using an iterative reconstruction method with measured attenuation correction, smoothed with an 8-mm gaussian filter. The reconstruction parameters were 28 subsets, 2 iterations in a 256×256 matrix

using a loop filter of 2.15-mm FWHM and a postfilter of 3.0-mm FWHM. Regional tumor radioactivity concentrations (%dose/mL) were estimated from the maximum pixels within regions of interest drawn around the tumor on transaxial slices of the reconstructed image sets.

Statistical Analysis

The statistical significance of comparisons between 2-h FIAU and either 2-h FHBG or 2-h FHPG values for RG2-TK+ and the ratios of RG2-TK+ to RG2 or muscle values was based on 2-sided paired Student *t* tests for matched values in the same rat. The statistical significance of comparisons between 2-h FIAU and 24-h FIAU values was based on 2-sided 2-sample *t* tests. Results are reported as mean \pm SD. Logarithmic transformations brought the data into closer agreement with implicit assumptions of normal statistical distributions with constant variance.

RESULTS

In Vitro Assays

A paired comparison of ^{14}C -FIAU, ^{18}F -FHBG, and ^{18}F -FHPG accumulation, normalized to ^3H -TdR in transduced RG2TK+ cells, is shown in Figure 1. The slopes of the plots show a 17-fold greater uptake of FIAU compared with that of FHBG and a 41-fold greater uptake of FIAU compared with that of FHPG. The mean values (\pm SD) of the tissue culture medium clearance constant (*K*) calculated for RG2TK+ cells were 0.38 ± 0.05 , 0.023 ± 0.001 , and 0.0077 ± 0.0004 mL/min/g cells for FIAU, FHBG, and FHPG, respectively. The mean *K* values for wild-type RG2 cells (data not shown) were much lower: 0.076 ± 0.013 , 0.0032 ± 0.0026 , and 0.0004 ± 0.0003 mL/min/g cells for FIAU, FHBG, and FHPG, respectively.

In Vivo Imaging

A comparison of ^{124}I -FIAU, ^{18}F -FHBG, and ^{18}F -FHPG PET images is shown in Figure 2. Each quadrant shows a

pair of images obtained from the same animal on sequential days. The 24-h FIAU images (animals 1 and 3) show localization of high levels of ^{124}I radioactivity in the transduced RG2TK+ xenograft and background levels of radioactivity in the contralateral RG2 wild-type xenograft (compared with shoulder muscles and thorax). Modest levels of radioactivity are also seen in the stomach, and lower levels of radioactivity are seen in the intestine. The corresponding 2-h FHBG (animal 1) images show low ^{18}F activity in the transduced RG2TK+ xenograft and background levels of radioactivity in the RG2 wild-type xenograft. The corresponding 2-h FHPG (animal 3) images show near-background ^{18}F activity in the transduced RG2TK+ xenograft and background levels of radioactivity in the RG2 wild-type xenograft. Xenograft localization to the shoulders was confirmed by the corresponding transmission scan images (e.g., animal 3 in Fig. 2). Background (thorax) radioactivity (%dose/g) was similar on the 2-h FHBG and FHPG images and on the 24-h FIAU images.

The comparison of a 2-h FHBG image with a corresponding 2-h FIAU image from animal 2 is shown in Figure 2. The FIAU radioactivity levels in the RG2TK+ xenografts at 2 and 24 h were similar (animals 1–3). The level of radioactivity in the RG2 xenograft was at background levels (e.g., shoulder muscles and thorax), although background radioactivity in nontransduced tissues was significantly higher at 2 h compared with that at 24 h (Table 1). Note the higher stomach radioactivity on the 2-h image (animal 2) compared with that at 24 h (animals 1 and 3). The corresponding 2-h FHBG images of animal 2 were similar to that observed in animal 1: low ^{18}F activity in the transduced RG2TK+ xenograft and background levels of radioactivity in the RG2 wild-type xenograft. However, gallbladder and intestine radioactivity on the 2-h FHBG images (animals 1

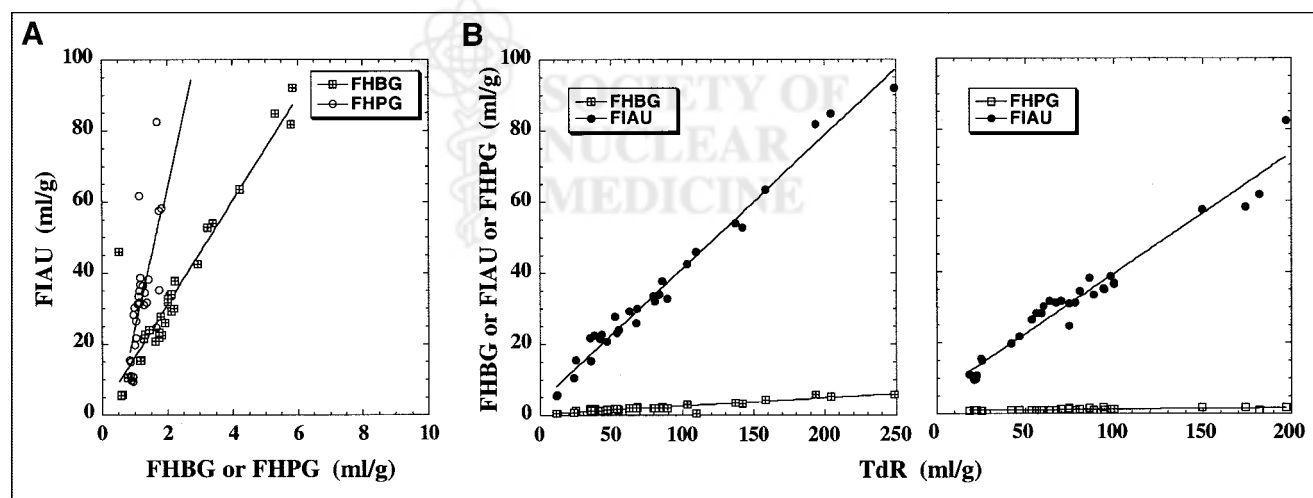


FIGURE 1. Paired nucleoside accumulation studies in RG2TK+ transduced cells. (A) ^{18}F -FHBG– ^{14}C -FIAU (■) and ^{18}F -FHPG– ^{14}C -FIAU (○) accumulation data (mL medium/g cells) are shown. (B) ^{18}F -FHBG– ^{14}C -FIAU and ^{18}F -FHPG– ^{14}C -FIAU comparisons with ^3H -TdR are shown: ^{14}C -FIAU (●), ^{18}F -FHBG (■), and ^{18}F -FHPG (□). Each point represents paired comparison of uptake results obtained from single triple-label experiment; experimental times varied between 10 and 180 min.

and 2) were substantially higher than that on the 2-h FIAU image (animal 2). Gallbladder and intestine radioactivity on the 2-h FHPG image (animal 3) was similar to that observed with FHBG (animals 1 and 2). Urinary bladder radioactivity at 2 h was high for all 3 probes; however, significant bladder

radioactivity was not observed on the 24-h FIAU images (animals 1 and 3). Background (shoulder muscles and thorax) radioactivity (%dose/g) on the 2-h FIAU images (animal 2, Fig. 2) was substantially greater than that on the 2-h FHBG and FHPG images.

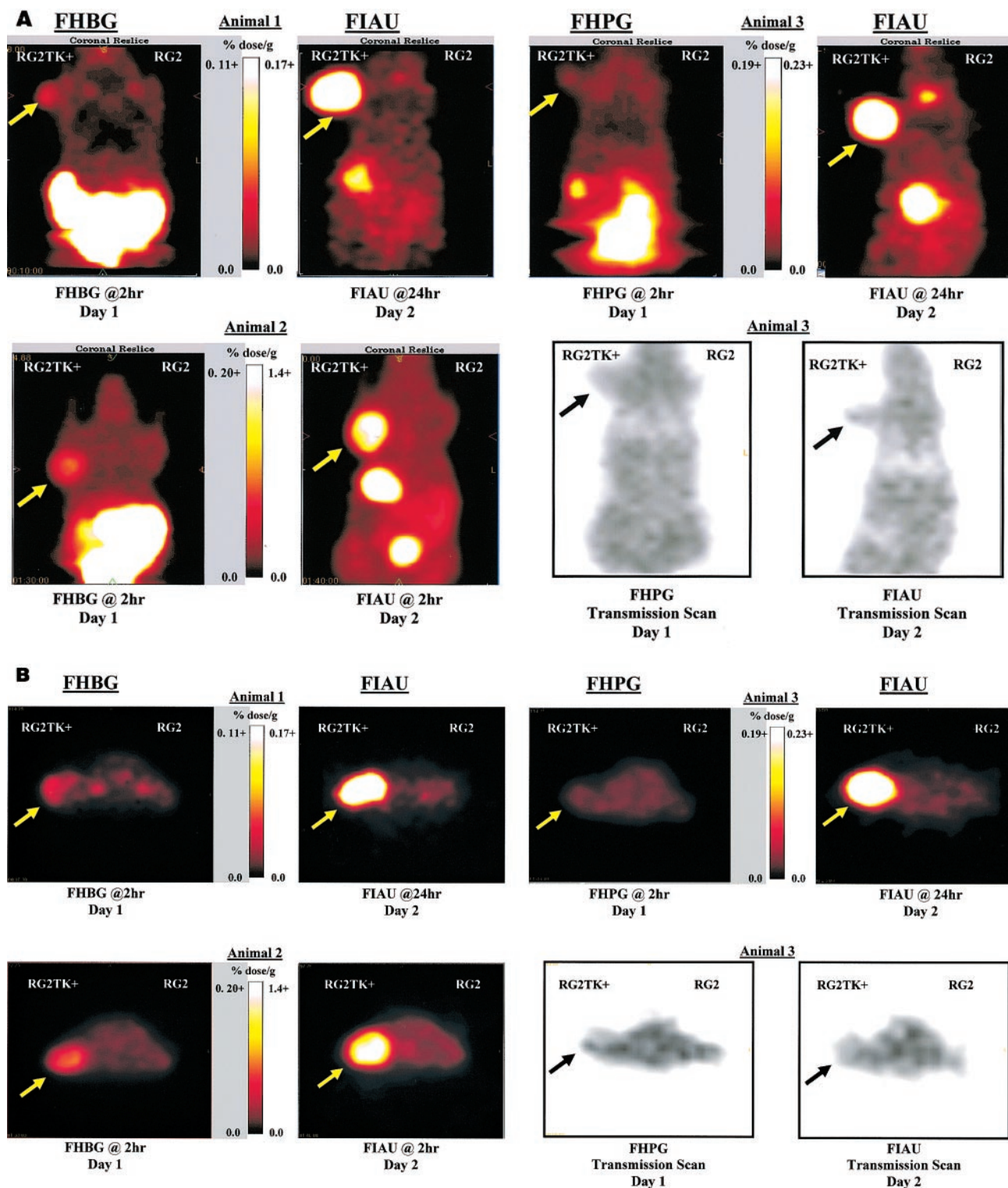


TABLE 1
Biodistribution of Different Probes for Imaging HSV1-*tk* Gene Expression

Tissue	FIAU, 2 h		FHBG, 2 h*		FHPG, 2 h*		FIAU, 24 h†	
	Mean ± SD	<i>n</i>	Mean ± SD	<i>n</i>	Mean ± SD	<i>n</i>	Mean ± SD	<i>n</i>
RG2TK+	1.217 ± 0.170	12	0.074 [‡] ± 0.049	6	0.023 [‡] ± 0.008	6	1.527 [§] ± 0.399	11
RG2	0.112 ± 0.042	12	0.013 [¶] ± 0.006	6	0.018 [¶] ± 0.005	6	0.026 [‡] ± 0.015	11
Plasma	0.244 ± 0.071	12	0.010 [¶] ± 0.003	6	0.043 [¶] ± 0.032	6	0.062 [‡] ± 0.035	11
Muscle	0.070 ± 0.015	12	0.016 [¶] ± 0.007	6	0.039 [¶] ± 0.025	6	0.015 [‡] ± 0.010	11
Liver	0.083 ± 0.028	12	0.026 [¶] ± 0.012	6	0.038 [¶] ± 0.020	6	0.018 [‡] ± 0.009	5
Stomach	0.137 ± 0.040	12	0.014 [¶] ± 0.004	6	0.016 [¶] ± 0.007	6	0.210 [§] ± 0.123	5
Heart	0.073 ± 0.017	12	0.006 [¶] ± 0.003	6	0.012 [‡] ± 0.004	6	0.011 [‡] ± 0.007	5
Lung	0.165 ± 0.045	12	0.013 [¶] ± 0.008	6	0.019 [‡] ± 0.005	6	0.028 [‡] ± 0.018	5
Kidney	0.249 ± 0.124	11	0.052 [¶] ± 0.061	6	0.079 [¶] ± 0.025	5	0.026 [‡] ± 0.018	5
Small intestine	0.170 ± 0.035	12	0.038 [¶] ± 0.025	6	0.029 [¶] ± 0.025	6	0.076 [‡] ± 0.026	5
Large intestine	0.170 ± 0.029	12	0.052 [¶] ± 0.027	6	0.035 [¶] ± 0.024	6	0.056 [‡] ± 0.014	5
Thyroid	0.125 ± 0.039	12	0.010 [¶] ± 0.004	6	0.016 [¶] ± 0.004	6	0.022 [‡] ± 0.014	5
Spleen	0.145 ± 0.047	12	0.021 [¶] ± 0.010	6	0.026 [‡] ± 0.009	6	0.027 [‡] ± 0.010	5
Brain	0.029 ± 0.007	12	0.0009 [¶] ± 0.0012	6	0.0027 [¶] ± 0.0012	6	0.0011 [‡] ± 0.0007	5

*Comparison of FHBG or FHPG vs. FIAU at 2 h by paired *t* test.

†Comparison of FIAU at 24 h vs. 2 h by unpaired *t* test.

‡*P* < 0.0001.

§*P* = not significant.

¶0.0001 < *P* < 0.0015.

||0.005 < *P* < 0.02.

Probability values are nominal significance levels for univariate tests unadjusted for multiple comparisons; *P* < 0.0001 and 0.0001 < *P* < 0.0015 remain significant even with conservative Bonferroni correction.

In Vivo Radioactivity Measurements

A comparison of FIAU, FHBG, and FHPG radioactivity (%dose/g) levels in different tissues is shown in Table 1. The xenograft tissue sampling data confirm the PET imaging findings; significantly higher levels of FIAU accumulate in RG2TK+ xenografts at 2 and 24 h compared with that of FHBG and FHPG at 2 h, and the differences between RG2TK+ and RG2 xenografts are highly significant. The difference in radioactivity between transduced RG2TK+ and wild-type RG2 xenografts and the paired RG2TK+/RG2 and RG2TK+/muscle concentration ratios are shown in Table 2. These differences and ratios were significantly greater for FIAU than for FHBG or FHPG. The FIAU radioactivity levels in RG2TK+ xenografts were similar in the 2- and 24-h experiments. However, the FIAU RG2TK+/RG2 and RG2TK+/muscle concentration ratios

were significantly higher at 24 h compared with those at 2 h because of the greater washout of background radioactivity over 24 h.

FIAU/FHBG and FIAU/FHPG concentration ratio comparisons in RG2TK+ and RG2 xenografts are shown in Table 3. In transduced RG2TK+ xenografts, FIAU accumulation was 20- and 60-fold higher than that of FHBG and FHPG, respectively, for the 2- and 24-h FIAU comparisons. In nontransduced, wild-type RG2 xenografts, the FIAU/FHBG and FIAU/FHPG ratios were 10-fold for the paired 2-h experiments; this was caused by the slower clearance of FIAU compared with that of FHBG and FHPG (Table 1). A comparison of the 24-h FIAU experiments with the 2-h FHBG and FHPG data for RG2 xenografts shows much smaller differences and a low concentration ratio, again indicating the slower body clearance of FIAU.

FIGURE 2. Paired PET imaging studies comparing ¹²⁴I-FIAU and ¹⁸F-FHBG or ¹⁸F-FHPG were performed. Coronal (A) and axial (B) PET images are shown for 3 different rats. Each animal had 2 imaging studies within 24 h, and comparable image pairs are shown in each quadrant of A and B. Location of RG2TK+ xenograft is indicated by arrow. Linear scaling of image intensity was performed to achieve similar background intensity on all images; background radioactivity in thorax was 0.013 and 0.027 %dose/g for animal 1, 0.024 and 0.18 %dose/g for animal 2, and 0.23 and 0.24 %dose/g for animal 3 (FHBG or FHPG and FIAU, respectively). No radioactivity above background is visualized in control RG2 xenograft. Several tissues had substantially higher values than indicated on intensity scale. For example, FIAU levels in RG2TK+ xenografts in animals 1–3 were 0.55, 1.7, and 1.2 %dose/g, respectively. Also note high values of radioactivity in stomach (6.0 %dose/g) and bladder (3.9 %dose/g) in 2-h study (animal 2). FHBG levels in abdominal viscera (2.8–3.2 %dose/g) and bladder (11 and 80 %dose/g) were also substantial at 2 h (animals 1 and 2); similar values were measured for FHPG in abdomen (3.4 %dose/g) and bladder (63 %dose/g) of animal 3. Note that FIAU bladder radioactivity had essentially cleared by 24 h (animals 1 and 3).

TABLE 2
Paired Comparisons of Probe Accumulation in HSV1-*tk* Transduced and Wild-Type RG2 Xenografts

Measurement	2 h*		2 h*		24 h*
	FIAU	FHBG	FIAU	FHPG	FIAU
Xenograft difference† (RG2TK+) – (RG2)	1.12 ± 0.16	0.062 ± 0.043	1.11 ± 0.19	0.006 ± 0.010	1.50 ± 0.69
Xenograft ratio‡ RG2TK+/RG2	11.3 ± 2.6	5.9 ± 2.3	8.9 ± 2.2	1.4 ± 0.7	65 ± 21
RG2TK+/muscle	18.1 ± 3.8	4.9 ± 2.2	16.9 ± 3.1	0.77 ± 0.44	124 ± 58

*Paired comparison from same animal tissue sampling dataset.

†Background-corrected RG2TK+ value. Difference expressed as %dose/g tissue.

‡Concentration ratio.

Paired 2-sample *t* tests of FIAU 2 h vs. FHBG 2 h or FIAU 2 h vs. FHPG 2 h for (RG2TK+) – (RG2), RG2TK+/RG2, RG2TK+/muscle: *P* < 0.0001. Unpaired, 2-sample *t* tests of FIAU 2 h vs. 24 h for RG2TK+/RG2, RG2TK+/muscle: *P* < 0.0001. Unpaired, 2-sample *t* tests of FIAU 2 h vs. 24 h for (RG2TK+) – (RG2): *P* = not significant.

Sequential Imaging (0–120 Minutes)

A comparison of 10-min imaging frames of ¹²⁴I-FIAU accumulation in a coronal section of a rat is shown in Figure 3. The sequence of images clearly reveals significant RG2TK+ activity above background in the initial 10-min frame. Although total body background is relatively high in the 10-min frame, it drops fairly rapidly with predominantly renal clearance. Also note that stomach activity builds rapidly and is greater than that in the RG2TK+ xenograft. The ¹²⁴I-FIAU accumulation profiles in RG2TK+ and RG2 xenografts are shown in Figure 4A. The corresponding accumulation profiles of ¹⁸F-FHBG from the same set of animals are shown in Figure 4B, and the accumulation profiles of ¹⁸F-FHPG from a different set of animals are shown in Figure 4C. FIAU accumulates rapidly and reaches a plateau in RG2TK+ xenografts during the 2-h period of imaging, whereas FIAU is being cleared from the RG2 xenograft. In contrast, FHBG and FHPG are being cleared from RG2TK+ transduced and wild-type xenografts over the 2-h imaging period. FHBG clearance from RG2TK+ xenografts appears to approach a plateau, whereas FHBG clearance from the RG2 xenografts and FHPG clearance from both xenografts fits a single exponential (there was no

significant difference between the FHPG profiles in RG2TK+ and RG2 xenografts).

The activity–time profiles of ¹²⁴I radioactivity (FIAU derived) in stomach and ¹⁸F radioactivity (FHPG derived) in intestine were assessed (data not shown). In 5 of 6 animals, ¹²⁴I radioactivity remained in the stomach; in 1 animal radioactivity was observed to move from stomach into the intestines during the 2-h imaging period. In all FHPG animals, the intestines contained the bulk of the ¹⁸F radioactivity; in 1 FHPG animal the kidneys were clearly observed. The hot spot of intestinal activity was observed to move from proximal (duodenal) to distal (large intestine) portions of the intestine during the 2-h period of imaging.

DISCUSSION

Several different radiolabeled probes have been developed and used to image HSV1-*tk* gene expression; these probes can be conveniently separated into pyrimidine nucleoside (e.g., FIAU, 2'-fluoro-2'-deoxy-5-iodo-1-β-D-ribofuranosyl-uracil [FIRU], 2'-fluoro-2'-5-methyl-1-β-D-arabinofuranosyl-uracil [FMAU], 2'-fluoro-2'-deoxy-5-iodovinyl-1-β-D-ribofuranosyl-uracil [IVFRU]) and acycloguanosine (e.g., 9-[(2-hydroxy-1-ethoxy)methyl]guanine [ACV], GCV, PCV, FGCV, FPCV, FHPG, FHBG) derivatives (Fig. 5). A listing of radiolabeled probes that have been developed for noninvasive PET imaging of HSV1-TK and a compilation of literature references relevant to probe comparisons are provided in Table 4. A major problem with comparing different radiolabeled pyrimidine nucleoside- and guanosine-based probes is that most studies only report a comparison between transduced and wild-type cells or xenografts and present no independent measure of HSV1-TK enzyme activity in the transduced cell line or tumor xenograft that is used to test efficacy. Because the level of HSV1-TK enzyme expression is likely to be different in the different transduced cells and tissue reported in the literature (Table 4), it is not possible to rigorously compare the results reported in many of the studies.

TABLE 3

Paired Comparisons of Probe Sensitivity and Specificity for Imaging HSV1-*tk* Expression

Xenograft measure*	2 h/2 h		24 h/2 h	
	FIAU/FHBG†	FIAU/FHPG†	FIAU/FHBG‡	FIAU/FHPG‡
RG2TK+	21 ± 10	59 ± 18	21	66
RG2	9.9 ± 3.3	9.8 ± 5.4	2.0	1.4

*Concentration ratio.

†Paired comparison from same animal tissue sampling dataset.

‡Ratio of mean values.

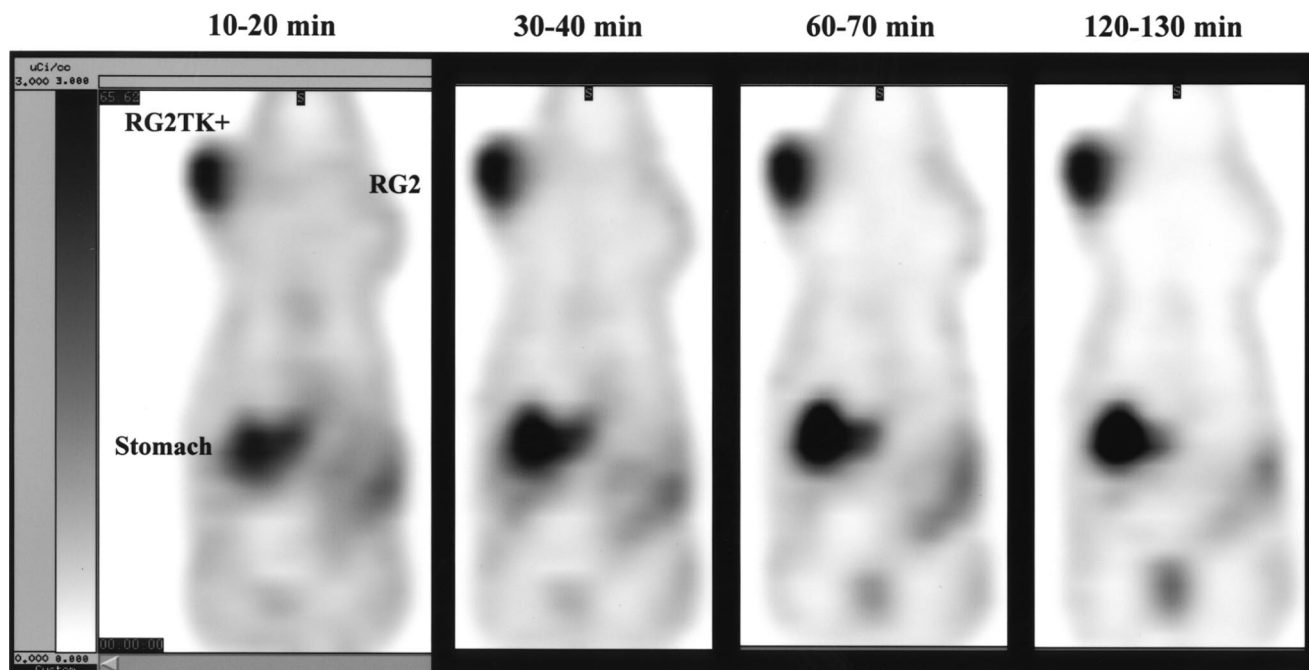


FIGURE 3. Comparison of 10-min imaging frames of FIAU accumulation. Ten-minute coronal image frames through RG2TK+ and RG2 xenografts are shown at various times after intravenous injection of ^{124}I -FIAU. Image intensity scale is same for all frames.

For example, HSV1-TK enzyme levels are likely to be higher after HSV1-*tk* gene transduction with adenoviral vectors at a high multiplicity of infection compared with that with retroviral vectors. Furthermore, it is usually not possible to normalize the data for the level of HSV1-TK activity in each test system (transduced cells or xenografts). Most comparisons are based on results obtained in different cell cultures or in different animals, and many are performed at different times. Thus, HSV1-TK probe efficacy comparisons derived from a review of the literature and a comparison of different studies are qualitative at best.

To address this issue, some investigators have performed sequential studies comparing 2 or more probes using the same transduced cell line or transduced xenograft. Alternatively, multilabel paired studies have been performed involving the simultaneous administration of 2 or more different radiolabeled probes to the same culture dish (1,12,14,15,24) or to the same xenograft-bearing animal (14,15,24). These studies provide the best direct in vitro and in vivo comparisons of different probes. On the basis of paired probe accumulation studies in HSV1-*tk* transduced cells performed in vitro (12,14,15,24), a comparison of

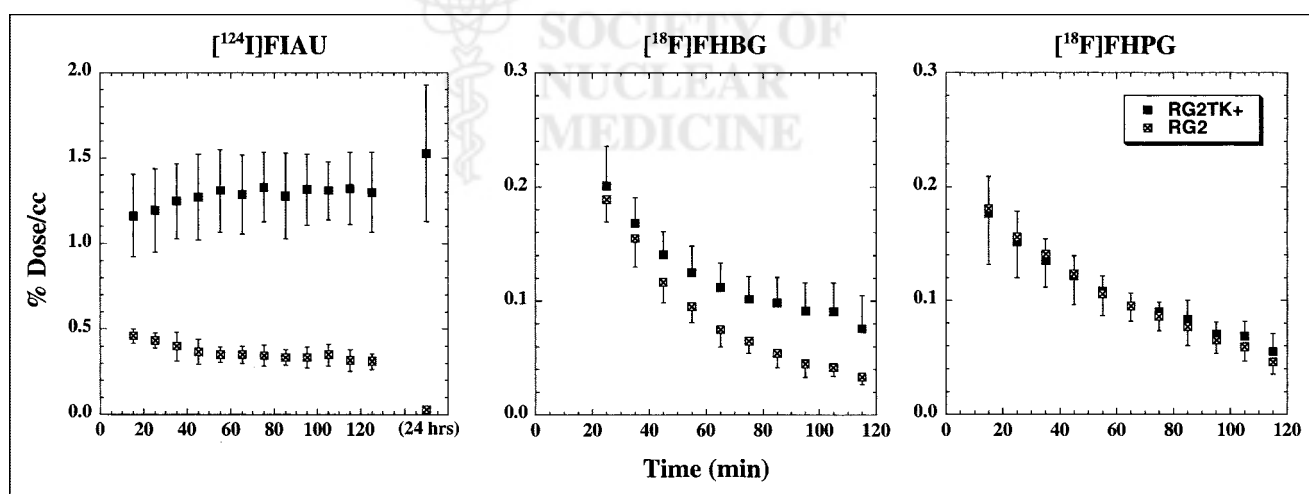


FIGURE 4. Radioactivity-time profiles in RG2TK+ and RG2 xenografts after intravenous injection of ^{124}I -FIAU, ^{18}F -FHBG, and ^{18}F -FHPG. Values (%dose/mL) are the mean \pm SD ($n = 6$) of maximum pixel value measured in each xenograft. FHBG and FIAU data were obtained from same set of animals imaged on consecutive days.

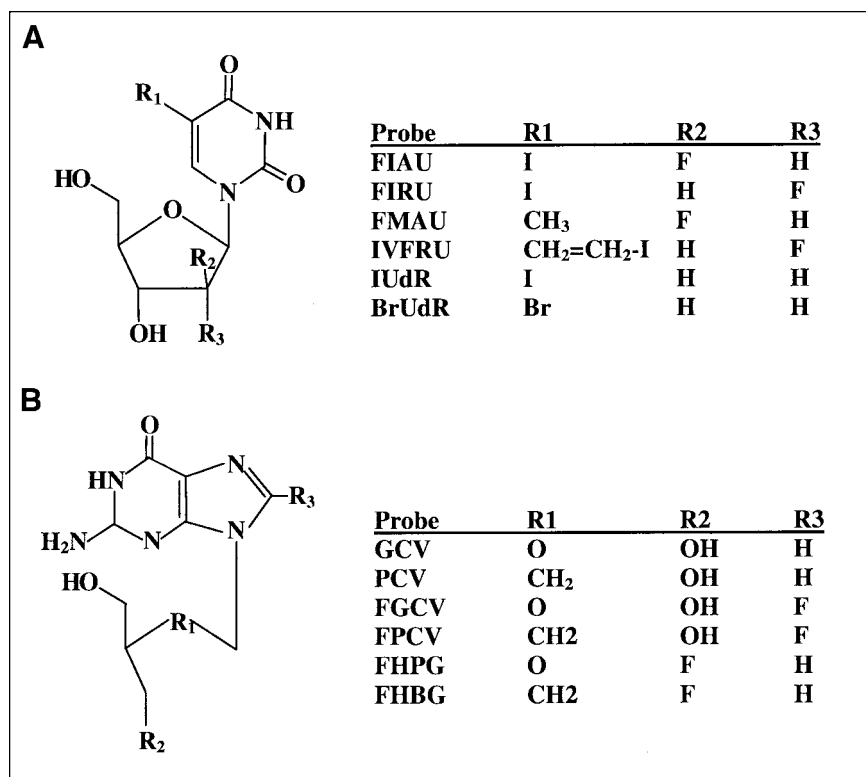


FIGURE 5. Chemical structures of pyrimidine (A) and acycloguanosine (B) nucleoside probes. IUdR = 2'-deoxy-5-iodo-1-β-D-ribofuranosyl-uracil; BrUdR = 2'-deoxy-5-bromo-1-β-D-ribofuranosyl-uracil.

values normalized to that of GCV (set at 1.0) yields the following nucleoside/GCV values: FGCV, ~0.5 (9,11); PCV, ~2.0 (12,14); FPCV, ~0.2 (14); FPCV, ~1.0 (15); FIAU, ~23 (1). Normalization of the in vitro data to acyclovir (which is accumulated in HSV1-*tk* transduced cells less avidly than GCV (11)) yields the following nucleoside/ACV values: FHPG, ~1–8, and FIAU, ~40–100; the FIAU/FHPG values varied between 5- and 100-fold (24). A direct comparison of the 2 probes in vivo showed that the FIAU/FHPG

ratio in HSV1-*tk* transduced tumors increased from 21 at 30 min to 119 at 4 h (24). Also note that FHPG cleared rapidly from the transduced tumor; a maximum of 2.2 ± 0.2 %dose/g was observed at 1 h, which fell to 0.2 ± 0.03 %dose/g at 4 h after injection. In contrast, FIAU remained essentially constant during this interval (12.7 ± 2.4 and 10.5 ± 3.9 %dose/g, respectively). Our results confirm this observation.

The objective of this study was to compare the efficacy of 3 radiolabeled probes of current interest (FIAU, FHBG, and

TABLE 4
Literature Summary of Probes for Imaging HSV1-*tk* Gene Expression

Radiolabeled probe	Chemical name	References
Pyrimidine derivatives		
FIAU (¹²³ I, ¹²⁴ I, ¹²⁵ I, ¹³¹ I)	2'-Fluoro-2'-deoxy-1-β-D-arabinofuranosyl-5-iodouracil	1–7, 22–24
FIRU (¹²⁵ I)	2'-Fluoro-2'-deoxy-5-iodo-1-β-D-ribofuranosyl-uracil	22, 23
FMAU (¹¹ C)	2'-Fluoro-2'-deoxy-5-methyl-1-β-D-arabinofuranosyl-uracil	25, 26
IVFRU (¹²³ I, ¹²⁵ I, ¹³¹ I)	2'-Fluoro-2'-deoxy-5-iodovinyl-1-β-D-ribofuranosyl-uracil	23, 27, 28
IUdR (³ H)	2'-Deoxy-5-iodo-1-β-D-ribofuranosyl-uracil (iododeoxyuridine)	1
Acycloguanosine derivatives		
ACV (8- ¹⁴ C, 8- ³ H)	9-[(2-Hydroxy-1-ethoxy)methyl]guanine (acyclovir)	11, 24
GCV (8- ¹⁴ C, 8- ³ H)	9-[(2-Hydroxy-1-(hydroxymethyl)ethoxy)methyl]guanine (ganciclovir)	1, 10, 11
PCV (8- ³ H)	9-[4-Hydroxy-3-(hydroxymethyl)butyl]guanine (penciclovir)	14, 15
FGCV (8- ¹⁸ F)	8-Fluoro-9-[(2-hydroxy-1-(hydroxymethyl)ethoxy)methyl]guanine (fluoroganciclovir)	12, 13
FPCV (8- ¹⁸ F)	8-Fluoro-9-[4-hydroxy-3-(hydroxymethyl)butyl]guanine (fluoropenciclovir)	14, 15
FHPG (3- ¹⁸ F)	9-[3-Fluoro-1-hydroxy-2-propoxymethyl]guanine	16, 17, 24, 25
FHBG (4- ¹⁸ F)	9-[4-Fluoro-3-(hydroxymethyl)butyl]guanine	18, 19, 29

References relate primarily to probe comparisons; because of reference number limitation, complete listing of all references was not possible.

FHPG) for in vivo imaging of HSV1-*tk* expression with PET. The in vitro and in vivo experimental design provided for paired comparisons between FIAU and FHBG and between FIAU and FHPG. The PET imaging comparisons were performed on the same animals on sequential days (within 24 h). The 2-h nucleoside accumulation comparisons were performed on the same tissue samples (animals) using double-label radiotracer techniques. These paired comparisons clearly show a 20-fold greater sensitivity of FIAU compared with that of FHBG for imaging HSV1-*tk* expression and a >50-fold sensitivity advantage for FIAU compared with that of FHPG.

The PET images revealed high levels of radioactivity in the viscera of the animals (Fig. 2), whereas comparatively low levels of radioactivity were measured in the tissue sampling experiments (Table 1). This apparent inconsistency is explained by the fact that almost all visceral radioactivity observed on the PET images of FIAU, FHBG, and FHPG was intraluminal, not in the wall of the viscera that were sampled for counting. The time course of FIAU- and FHPG-derived radioactivity in stomach and intestine was assessed (data not presented). ^{124}I radioactivity remained largely in the stomach, whereas ^{18}F radioactivity was observed to rapidly move through the intestine. The hepatobiliary route of excretion of ^{18}F -acycloguanosine derivatives has been well documented (12–19,24,25,32).

The issue of metabolic degradation and presence of radiolabeled metabolites was not addressed in this study. It has been shown that FIAU is resistant to metabolic degradation (29); pharmacologic doses of FIAU are excreted largely unchanged through the kidney and urine in patients (30). However, the intraluminal localization of radioactivity to stomach and to thyroid in animals not receiving a blocking dose of iodide indicates some deiodination of tracer ^{124}I -FIAU in vivo. GCV and other acycloguanosine analogs are also resistant to metabolic degradation (48). ^{18}F -FGCV, ^{18}F -FPCV, and ^{18}F -FHPG have been shown to be metabolically stable in blood and liver (17,19,20,22), and studies on healthy volunteers and primates indicate that ^{18}F -FHBG is excreted largely unchanged in the urine (19,32). Further studies specifically addressing the issue of radiolabeled metabolites in blood and tissue need to be performed.

Another issue that has not been addressed in this study or earlier HSV1-*tk* imaging studies is whether probe transport across cell and tissue membranes is limiting and affects the images. Nucleosides are polar, and several classes of equilibrative (33) and concentrative (34) nucleoside transporters have been identified in cell membranes. The Na^+ -dependent concentrative transporters are expressed primarily in epithelial cells and proliferating tissues; they have been characterized as purine selective (N1, SPNT, or CNT2), pyrimidine selective (N2, CNT1), and broadly selective (N3, N4, and N5) (34). Although the data are indirect, there appears to be a wide range of nucleoside transporters expressed in different cell lines and tissue (organs) (35,36) as well as depressed levels of expression in some tumors (36). Trans-

port limitations may affect the acycloguanosine compounds more than the pyrimidine nucleoside derivatives (10,24,25). If nucleoside (probe) transport is a rate-determining step for probe accumulation in HSV1-*tk* transduced cells and tissue, nucleoside transporter expression could affect the images and account for some of the variability reported in the literature (10,24). Detailed transport studies comparing different acycloguanosine and pyrimidine nucleoside probes have not been reported, although modification of the 3'-position, loss of the 3'-hydroxyl, loss of a portion of the sugar ring, and lack of conformational flexibility are factors that significantly decrease the affinity of some nucleoside analogs to nucleoside transporters, which results in a decreased transport into the cells (10,37).

It has not been resolved whether nucleoside (probe) transport across cell membranes significantly affects net accumulation of radioactivity (and intensity of the images) in HSV1-*tk*-expressing tissue. Rapid accumulation of FIAU in RG2TK+ xenografts is revealed in the early (10–20 min) image frames (Figs. 3 and 4), and this is encouraging. Also note that initial 2-min-duration emission scans were obtained as scout views (~5–10 min after intravenous injection of the radiolabeled probes), and they provided good quality images of the RG2TK+ xenograft in animals injected with FIAU but not with FHBG or FHPG. This suggests that cell membrane transport may not be limiting for FIAU; further in vivo and in vitro kinetic studies are needed to establish this point.

The results of the paired 2-h studies clearly show the sensitivity and dynamic range advantages of FIAU over FHBG or FHPG for imaging HSV1-*tk* expression. The ability to image late, ≥ 24 h after FIAU administration, also provides the opportunity to achieve high image specificity because of physiologic washout of background radioactivity and the retention of the radioactivity in HSV1-*tk* transduced tissue (1–3). Although FIAU is usually labeled with ^{124}I for PET studies (or with ^{123}I or ^{131}I for gamma-camera scintigraphy) and late imaging is usually performed, our results show the feasibility of early FIAU imaging. Good quality images can be obtained within the first 30 min to 2 h after FIAU administration (Figs. 2–4). Thus, radiolabeling FIAU with ^{18}F or ^{11}C is an alternative strategy to using FHBG or FHPG; it would provide additional positron-emitting FIAU probes with high HSV1-*tk* sensitivity and dynamic range. In addition, the relatively short half-life of these radionuclides would facilitate repeated or sequential PET imaging of HSV1-*tk* expression.

To enhance the HSV1-*tk* imaging sensitivity of radiolabeled acycloguanosine probes, the use of site-mutated variants of wild-type HSV1-*tk* as the reporter gene has been proposed recently (14). This proposal developed from earlier work that showed enhanced ganciclovir and acyclovir cytotoxicity and enhanced drug phosphorylation with site-mutated HSV1-*tk* variants compared with wild-type HSV1-*tk* (38,39). Initial results obtained with the HSV1-*sr39tk* mutant (generated by semirandom sequence mu-

tagenesis) revealed enhanced sensitivity for PCV and FPCV, but this enhancement was modest (~ 2 -fold) (14). Furthermore, the ~ 2 -fold enhancement in probe accumulation contrasts with the ~ 300 -fold difference in GCV 50% inhibitory concentration (IC_{50}) between HSV1-*sr39tk* and wild-type HSV1-*tk* C6 transfectants (39). This disparity raises the question of whether cell membrane transport of PCV and FPCV was limiting in the radiolabeled probe accumulation studies run over a period of 15–240-min (14); in contrast, the GCV IC_{50} studies were run over a 3-d period, providing a longer period for GCV to enter the cell and exert a cytotoxic effect (38–40). Our previous GCV uptake studies in tissue culture were run over a 24-h period and the cell/medium concentration ratios were initially low in RG2 and RG2TK+ cells (1): at 1 h, the GCV ratios (uncorrected for cell-adherent medium) were 0.68 ± 0.12 and 0.64 ± 0.21 mL/g for RG2 and RG2TK+ cells, respectively; at 4 h, the ratios were 0.70 ± 0.16 and 0.97 ± 0.35 mL/g, respectively; at 8 h, the ratios were 0.69 ± 0.10 and 1.17 ± 0.08 mL/g, respectively; and at 24 h, the ratios were 0.94 ± 0.09 and 2.8 ± 1.0 mL/g, respectively. The K values for GCV were 0.00020 ± 0.00004 mL/min/g cells in RG2 cells and 0.00156 ± 0.00009 mL/min/g cells in RG2TK+ cells (values determined from data presented in (1)) and are consistent with slow GCV equilibration across RG2 and RG2TK+ cell membranes. An approximation of the probe-cell equilibration times in vitro can be obtained from the reciprocal of the K values; for FIAU, FHBG, FHPG, and GCV flux into RG2TK+ cells, the calculated values are 2.6, 43, 130, and 641 min, respectively. Thus, cell membrane transport could be a factor in limiting FHBG, FHPG, and GCV accumulation in transduced cells.

The sensitivity and dynamic range of a PET reporter probe are important considerations that will impact on animal and patient studies. Our data clearly show the advantages of FIAU compared with FHBG and FHPG. Greater sensitivity and dynamic range provide the ability to image lower levels of reporter gene expression over a wider range of expression levels. This advantage translates into several practical benefits: Lower quantities of vector are required for successful transduction of target tissue with the reporter system, a wider range of image intensity is provided for more accurate quantitation of reporter expression, and a more sensitive measure of weakly activated reporter systems is provided. For example, the higher sensitivity and wider dynamic range of PET imaging with FIAU allows more accurate monitoring of small changes in the activity of various signal-transduction pathways, when expression of the HSV1-*tk* reporter gene is controlled by a signal-transduction specific *cis*-acting promoter/enhancer element. Our recent studies showed that the p53 signal-transduction pathway activity in tumors could be imaged successfully with ^{124}I -FIAU and PET when the HSV1-*tk* gene was placed under control of an artificial *cis*-acting p53-specific promoter (6). In another study, we showed that highly specific images of T-cell activation could be obtained when the

HSV1-*tk* gene was placed under control of an artificial *cis*-acting promoter that is specific to the nuclear factor of activated T-cells (7).

Looking ahead to the clinical application of these reporter systems, it is necessary to consider the differences in maximum allowable injected dose of the reporter substrate, the differences in the rates of decay of the radiolabels, and, for PET imaging, the differences in positron abundance. Except for FHBG (19,32), detailed dosimetry studies in humans or primates have not been reported for these tracers. The biodistribution and dosimetry in healthy subjects after intravenous administration of 70–229 MBq (1.9–6.2 mCi) ^{18}F -FHBG showed that the urinary bladder wall was the dose-limiting organ: 0.094 mGy/MBq (0.35 rad/mCi) (19). If the dose limitations are similar to those of other tracers labeled with the same radioisotopes (namely, an ~ 5 -mCi maximum for ^{124}I and an ~ 10 mCi maximum for ^{18}F), the following comparisons could be made. The 2:1 advantage of the ^{18}F -labeled probes over the ^{124}I - probes is further extended to 8:1 when positron abundance (23% for ^{124}I and 98% for ^{18}F) is considered but is back to 4:1 for imaging at 2 h because of decay. However, even when this 4:1 advantage in counts for ^{18}F over ^{124}I is considered, the positron signal from ^{124}I -FIAU is still expected to be significantly higher than that from either ^{18}F -FHBG or ^{18}F -FHPG. Furthermore, note that the ratios of transduced to nontransduced tissues are not affected by these considerations, and the image contrast would be expected to be similar to that observed in this study.

CONCLUSION

Our results show that FIAU is a substantially better probe than either FHBG or FHPG for imaging HSV1-*tk* expression, with greater sensitivity and dynamic range as well as lower abdominal background radioactivity at 2 and 24 h. Reasonably good FIAU images were obtained as early as 10 min after intravenous injection, and a plateau of retained FIAU-derived radioactivity is reached during the 2-h imaging period after injection. In contrast, FHBG and FHPG are being cleared from transduced and wild-type xenografts over the 2-h imaging period after injection. FHBG appears to approach a plateau and be retained in RG2TK+ xenografts after ≥ 2 h, whereas FHPG clearance is exponential. Abdominal background activity of FHBG was greater than that of FHPG because of the more rapid hepatobiliary clearance of FHBG. Transport across cell membranes may be a rate-limiting process for imaging HSV1-*tk* expression with radiolabeled acycloguanosine probes, but this does not appear to be the case for radiolabeled FIAU.

ACKNOWLEDGMENTS

The authors thank Bradley Beattie and Steven Larson (Memorial Sloan-Kettering Cancer Center) for their help and generous support. The single-crystal FIAU x-ray analysis was performed by Gerard Parkin and Joseph Tanski (Department of Chemistry, Columbia University). This

work was supported by National Institutes of Health grants P50 CA86438, CA98023, CA57599, CA76117, and CA83084 and by Department of Energy grant FG03-86ER60407.

REFERENCES

- Tjuvajev JG, Stockhammer G, Desai R, et al. Imaging the expression of transfected genes in vivo. *Cancer Res.* 1995;55:6126–6132.
- Tjuvajev JG, Finn R, Watanabe K, et al. Noninvasive imaging of herpes virus thymidine kinase gene transfer and expression: a potential method for monitoring clinical gene therapy. *Cancer Res.* 1996;56:4087–4095.
- Tjuvajev JG, Finn R, Watanabe K, et al. Imaging herpes virus thymidine kinase gene transfer and expression by positron emission tomography. *Cancer Res.* 1998;58:4333–4341.
- Tjuvajev JG, Joshi A, Callegari J, et al. A general approach to the non-invasive imaging of transgenes using cis-linked herpes simplex virus thymidine kinase. *Neoplasia.* 1999;1:315–320.
- Tjuvajev JG, Chen SH, Joshi A, et al. Imaging adenoviral-mediated herpes virus thymidine kinase gene transfer and expression in vivo. *Cancer Res.* 1999;59:5186–5193.
- Dobrovinn M, Ponomarev V, Beresten T, et al. Imaging transcriptional regulation of p53 dependent genes in vivo with positron emission tomography. *Proc Natl Acad Sci USA.* 2001;98:9300–9305.
- Ponomarev V, Dobrovinn M, Lyddane C, et al. Imaging TCR-dependent NFAT-mediated T-cell activation with positron emission tomography in vivo. *Neoplasia.* 2001;3:480–488.
- Iyer M, Wu L, Carey M, et al. Two-step transcriptional amplification as a method for imaging reporter gene expression using weak promoters. *Proc Natl Acad Sci USA.* 2001;98:14595–14600.
- Yu Y, Annala AJ, Barrio JR, et al. Quantification of target gene expression by imaging reporter gene expression in living animals. *Nat Med.* 2000;6:933–937.
- Haberkorn U, Khazaie K, Morr I, et al. Ganciclovir uptake in human mammary carcinoma cells expressing herpes simplex virus thymidine kinase. *Nucl Med Biol.* 1998;25:367–373.
- Gambhir SS, Barrio JR, Wu L, et al. Imaging of adenoviral-directed herpes simplex virus type 1 thymidine kinase reporter gene expression in mice with radiolabeled ganciclovir. *J Nucl Med.* 1998;39:2003–2011.
- Gambhir SS, Barrio JR, Phelps ME, et al. Imaging adenoviral-directed reporter gene expression in living animals with positron emission tomography. *Proc Natl Acad Sci USA.* 1999;96:2333–2338.
- Namavari M, Barrio JR, Toyokuni T, et al. Synthesis of 8-[¹⁸F]fluoroguanine derivatives: in vivo probes for imaging gene expression with positron emission tomography. *Nucl Med Biol.* 2000;27:157–162.
- Gambhir SS, Bauer E, Black ME, et al. A mutant herpes simplex virus type 1 thymidine kinase reporter gene shows improved sensitivity for imaging reporter gene expression with positron emission tomography. *Proc Natl Acad Sci USA.* 2000;97:2785–2790.
- Iyer M, Barrio JR, Namavari M, et al. 8-[¹⁸F]Fluoropenciclovir: an improved reporter probe for imaging HSV1-tk reporter gene expression in vivo using PET. *J Nucl Med.* 2001;42:96–105.
- Alauddin MM, Conti PS, Mazza SM, et al. 9-[(3-[¹⁸F]-Fluoro-1-hydroxy-2-propoxy)methyl]guanine ([¹⁸F]-FHPG): a potential imaging agent of viral infection and gene therapy using PET. *Nucl Med Biol.* 1996;23:787–792.
- Alauddin MM, Shahinian A, Kundu RK, et al. Evaluation of 9-[(3-[¹⁸F]-fluoro-1-hydroxy-2-propoxy)methyl]guanine ([¹⁸F]-FHPG) in vitro and in vivo as a probe for PET imaging of gene incorporation and expression in tumors. *Nucl Med Biol.* 1999;26:371–376.
- Alauddin MM, Conti PS. Synthesis and preliminary evaluation of 9-(4-[¹⁸F]-fluoro-3-hydroxymethylbutyl)guanine ([¹⁸F]FHBG): a new potential imaging agent for viral infection and gene therapy using PET. *Nucl Med Biol.* 1998;25:175–180.
- Yaghoubi S, Barrio JR, Dahlbom M, et al. Human pharmacokinetic and dosimetry studies of [¹⁸F]FHBG: a reporter probe for imaging herpes simplex virus type-1 thymidine kinase reporter gene expression. *J Nucl Med.* 2001;42:1225–1234.
- Sheh Y, Kozirowski J, Balatoni J, et al. Low energy cyclotron production and chemical separation of “no carrier added” iodine-124 from a reusable, enriched tellurium-124 dioxide/aluminum oxide solid solution target. *Radiochim Acta.* 2000;88:169–173.
- Vaidyanathan G, Larsen RH, Zalutsky MR. 5-[²¹¹At]Astatato-2'-deoxyuridine, an α -particle-emitting eudoradiotherapeutic agent undergoing DNA incorporation. *Cancer Res.* 1996;56:1204–1209.
- Tovell DR, Samuel J, Mercer JR, et al. The in vitro evaluation of nucleoside analogues as probes for use in the noninvasive diagnosis of herpes simplex encephalitis. *Drug Des Deliv.* 1988;3:213–221.
- Wiebe LI, Knaus EE, Morin KW. Radiolabelled pyrimidine nucleosides to monitor the expression of HSV-1 thymidine kinase in gene therapy. *Nucleosides Nucleotides.* 1999;18:1065–1066.
- Brust P, Haubner R, Friedrich A, et al. Comparison of [¹⁸F]FHPG and [¹²⁴I/125I]FIAU for imaging herpes simplex virus type 1 thymidine kinase gene expression. *Eur J Nucl Med.* 2001;28:721–729.
- de Vries EF, van Waarde A, Harmsen MC, et al. [¹¹C]FMAU and [¹⁸F]FHPG as PET tracers for herpes simplex virus thymidine kinase enzyme activity and human cytomegalovirus infections. *Nucl Med Biol.* 2000;27:113–119.
- Bading JR, Shahinian AH, Bathija P, Conti PS. Pharmacokinetics of the thymidine analog 2'-fluoro-5-[¹⁴C]-methyl-1-beta-D-arabinofuranosyluracil ([¹⁴C]FMAU) in rat prostate tumor cells. *Nucl Med Biol.* 2000;27:361–368.
- Morin KW, Atrazheva ED, Knaus EE, Wiebe LI. Synthesis and cellular uptake of 2'-substituted analogues of (E)-5-(2-[¹²⁵I]iodovinyl)-2'-deoxyuridine in tumor cells transduced with the herpes simplex type-1 thymidine kinase gene: evaluation as probes for monitoring gene therapy. *J Med Chem.* 1997;40:2184–2190.
- Morin KW, Knaus EE, Wiebe LI, et al. Reporter gene imaging: effects of ganciclovir treatment on nucleoside uptake, hypoxia and perfusion in a murine gene therapy tumour model that expresses herpes simplex type-1 thymidine kinase. *Nucl Med Commun.* 2000;21:129–137.
- Machida H, Watanabe Y, Kano F, et al. Deglycosylation of antiherpes viral 5-substituted arabinosyluracil derivatives by rat liver extract and enterobacteria cells. *Biochem Pharmacol.* 1995;49:763–766.
- Feinberg A, Leyland-Jones B, Fanucchi MP, et al. Biotransformation and elimination of 2-[¹⁴C]-5-iodo-(2'-fluoro-2'-deoxy-1- β -D-arabino-furanosyl)-cytosine in immuno-suppressed patients with herpesvirus infections. *Antimicrob Agents Chemother.* 1985;27:733–738.
- Faulds D, Heel RC. Ganciclovir: a review of its antiviral activity, pharmacokinetic properties and therapeutic efficacy in cytomegalovirus infections. *Drugs.* 1990;39:597–638.
- Alauddin MM, Shahinian A, Gordon EM, et al. Preclinical evaluation of the penciclovir analog 9-(4-[¹⁸F]fluoro-3-hydroxymethylbutyl)guanine for in vivo measurement of suicide gene expression with PET. *J Nucl Med.* 2001;42:1682–1690.
- Hyde RJ, Cass CE, Young JD, Baldwin SA. The ENT family of eukaryote nucleoside and nucleobase transporters: recent advances in the investigation of structure/function relationships and the identification of novel isoforms. *Mol Membr Biol.* 2001;18:53–63.
- Ritzel MW, Ng AM, Yao SY, et al. Recent molecular advances in studies of the concentrative Na⁺-dependent nucleoside transporter (CNT) family: identification and characterization of novel human and mouse proteins (hCNT3 and mCNT3) broadly selective for purine and pyrimidine nucleosides (system cib). *Mol Membr Biol.* 2001;18:65–72.
- Cass CE, Young JD, Baldwin SA, et al. Nucleoside transporters of mammalian cells. *Pharm Biotechnol.* 1999;12:313–352.
- Pastor-Anglada M, Casado FJ, Valdes R, Mata J, Garcia-Manteiga J, Molina M. Complex regulation of nucleoside transporter expression in epithelial and immune system cells. *Mol Membr Biol.* 2001;18:81–85.
- Gati WP, Misra HK, Knaus EE, Wiebe LI. Structural modifications at the 2'- and 3'-positions of some pyrimidine nucleosides as determinants of their interaction with the mouse erythrocyte nucleoside transporter. *Biochem Pharmacol.* 1984;33:3325–3331.
- Black ME, Newcomb TG, Wilson HM, Loeb LA. Creation of drug-specific herpes simplex virus type 1 thymidine kinase mutants for gene therapy. *Proc Natl Acad Sci USA.* 1996;93:3525–3529.
- Black ME, Kokoris MS, Sabo P. Herpes simplex virus-1 thymidine kinase mutants created by semi-random sequence mutagenesis improve prodrug-mediated tumor cell killing. *Cancer Res.* 2001;61:3022–3026.
- Haberkorn U, Altmann A, Morr I, et al. Monitoring gene therapy with herpes simplex virus thymidine kinase in hepatoma cells: uptake of specific substrates. *J Nucl Med.* 1997;38:287–294.



The Journal of
NUCLEAR MEDICINE

Comparison of Radiolabeled Nucleoside Probes (FIAU, FHBG, and FHPG) for PET Imaging of HSV1- *tk* Gene Expression

Juri Gelovani Tjuvaje, Mikhail Doubrovin, Timothy Akhurst, Shangde Cai, Julius Balatoni, Mian M. Alauddin, Ronald Finn, William Bornmann, Howard Thaler, Peter S. Conti and Ronald G. Blasberg

J Nucl Med. 2002;43:1072-1083.

This article and updated information are available at:
<http://jnm.snmjournals.org/content/43/8/1072>

Information about reproducing figures, tables, or other portions of this article can be found online at:
<http://jnm.snmjournals.org/site/misc/permission.xhtml>

Information about subscriptions to JNM can be found at:
<http://jnm.snmjournals.org/site/subscriptions/online.xhtml>

The Journal of Nuclear Medicine is published monthly.
SNMMI | Society of Nuclear Medicine and Molecular Imaging
1850 Samuel Morse Drive, Reston, VA 20190.
(Print ISSN: 0161-5505, Online ISSN: 2159-662X)

© Copyright 2002 SNMMI; all rights reserved.